Solitons and exact velocity quantization of incommensurate sliders

2007 J. Phys.: Condens. Matter 19 305016

(http://iopscience.iop.org/0953-8984/19/30/305016)

IOP PUBLISHING JOURNAL OF PHYSICS: CONDENSED MATTER

J. Phys.: Condens. Matter **19** (2007) 305016 (10pp) doi:10.1088/0953-8984/19/30/305016

Solitons and exact velocity quantization of incommensurate sliders

Nicola Manini[1,2], Marco Cesaratto[1,2], Giuseppe E Santoro[2,3,4], Erio Tosatti[2,3,4] and Andrea Vanossi[5]

[1] Dipartimento di Fisica and CNR-INFM, Università di Milano, Via Celoria 16, 20133 Milano, Italy
[2] International School for Advanced Studies (SISSA), Via Beirut 2-4, I-34014 Trieste, Italy
[3] INFM Democritos National Simulation Center, Via Beirut 2-4, I-34014 Trieste, Italy
[4] International Centre for Theoretical Physics (ICTP), PO Box 586, I-34014 Trieste, Italy
[5] CNR-INFM National Research Center S3 and Department of Physics, University of Modena and Reggio Emilia, Via Campi 213/A, 41100 Modena, Italy

Received 5 February 2007, in final form 26 February 2007
Published 13 July 2007
Online at stacks.iop.org/JPhysCM/19/305016

Abstract

We analyse in some detail the recently discovered velocity quantization phenomena in the classical motion of an idealized one-dimensional solid lubricant, consisting of a harmonic chain interposed between two periodic sliders. The ratio $w = v_{cm}/v_{ext}$ of the chain centre-of-mass velocity to the externally imposed relative velocity of the sliders is pinned to exact 'plateau' values for wide ranges of parameters, such as sliders corrugation amplitudes, external velocity, chain stiffness and dissipation, and is strictly determined by the commensurability ratios alone. The phenomenon is caused by one slider rigidly dragging the density solitons (kinks/antikinks) that the chain forms with the other slider. Possible consequences of these results for some real systems are discussed.

(Some figures in this article are in colour only in the electronic version)

1. Introduction to the model

The sliding friction of hard incommensurate crystals has stimulated for over a decade the study of nonlinear classical dynamical systems—belonging to the class of generalized Frenkel–Kontorova (FK) models [1]—which can show a rich variety of dynamical behaviour, ranging from regular to chaotic motion [2]. In particular, in the presence of uniform external driving, the length-scale competition between different spatial periodicities can give rise to intriguing frequency incommensurations and phase locking phenomena. In this paper we discuss and analyse in depth the striking exact velocity quantization phenomena recently reported in a one-dimensional (1D) nonlinear model inspired by the tribological problem of two sliding surfaces with a thin solid lubricant layer in between [3, 4]. The model 'layer' consists here

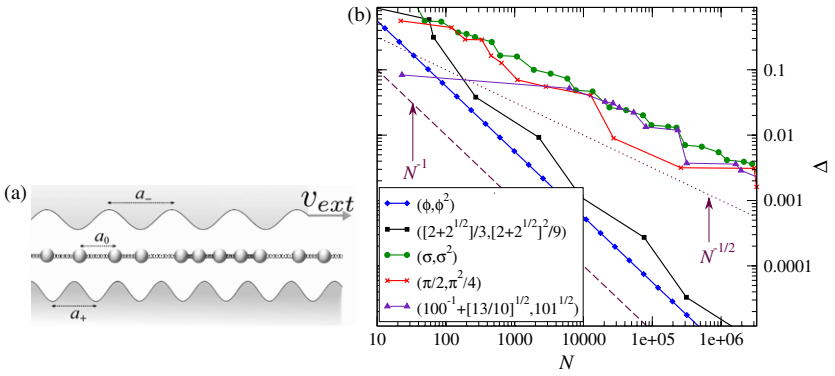

Figure 1. (a) A sketch of the model with the two periodic sliders (periods a_+ and a_-) and the lubricant harmonic chain of rest nearest-neighbour length a_0. (b) The finite-size phase error Δ of equation (2) (only the N values where Δ is smaller than for any other $N' < N$ are shown) decreases as a function of size N. Note that the error drops fast as N^{-1} for golden mean and other quadratic incommensurabilities (r_+, $r_- = r_+^2$), but slowly as $N^{-1/2}$ for spiral mean and other non-quadratic incommensurabilities.

Table 1. Natural units for several physical quantities in a system where length, force and mass are measured in units of a_+, F_+, and m, respectively.

Energy	$a_+ F_+$
Velocity, v	$a_+^{1/2} F_+^{1/2} m^{-1/2}$
Time	$a_+^{1/2} F_+^{-1/2} m^{1/2}$
Spring constant, K	$a_+^{-1} F_+$
Viscous friction, γ	$a_+^{-1/2} F_+^{1/2} m^{1/2}$

of a chain of N harmonically interacting particles interposed between two rigid generally (but not necessarily) incommensurate sinusoidal substrates representing the two 'sliding crystals', sketched in figure 1(a), externally driven at a constant relative velocity $v_{\rm ext}$. The equation of motion of the ith particle is:

$$m\ddot{x}_i = -\tfrac{1}{2}\left[F_+ \sin k_+(x_i - v_+ t) + F_- \sin k_-(x_i - v_- t)\right] + K(x_{i+1} + x_{i-1} - 2x_i) - \gamma \sum_{\pm}(\dot{x}_i - v_\pm), \tag{1}$$

where m is the mass of the N particles, K is the chain spring constant, and $k_\pm = (2\pi)/a_\pm$ are the wavevector periodicities of potentials representing the two sliders, moving at velocities $v_\pm$. We choose the reference frame where $v_+ = 0$, so that $v_{\rm ext} \equiv v_- - v_+ = v_-$. γ is a phenomenological parameter substituting for various sources of dissipation. Dissipation is required to achieve a stationary state, but has otherwise no major role in the following. $F_\pm$ are the amplitudes of the forces representing the sinusoidal corrugation of the two sliders (we will commonly use $F_-/F_+ = 1$, but we did check that our results are more general). We take $a_+ = 1$, $m = 1$, and $F_+ = 1$ as our basic units, so that the natural units for all quantities used to characterize the model are listed in table 1.

The relevant length ratios [5, 6] are therefore $r_\pm = a_\pm/a_0$; we take, without loss of generality, $r_- > r_+$. The inter-particle equilibrium length a_0, not entering explicitly the equation of motion (1), appears via the boundary conditions, which are taken to be periodic (PBC), $x_{N+1} = x_1 + Na_0$, to enforce a fixed-density condition for the chain [1], with a *coverage* r_+ of chain atoms on the 'denser' substrate of periodicity a_+. Technically, the PBCs

can be realized in two different manners. The first (i) is quite standard [1], and consists of approximating r_+ and r_- with suitable rational numbers N/N_+ and N/N_- (with $N_\pm = [N/r_\pm]$ meaning the nearest integer of $N/r_\pm$). The second (ii) uses, instead, a finite N and machine-precision values of r_+ and r_-. For irrational r_+ and/or r_-, both methods introduce a finite-size error

$$\Delta = \Delta_+ + \Delta_-, \qquad \text{with } \Delta_\pm = 2\pi \left| N_\pm - \frac{N}{r_\pm} \right|, \tag{2}$$

in the relative phase of the three periodic objects involved in the model. In method (i) this error is distributed uniformly through the chain, while in method (ii) it remains concentrated where the boundary condition applies, at sites 1 and N. For a generic N, Δ is of order unity, but, as illustrated in figure 1(b) (reporting the N values where Δ is smaller than for any other $N' < N$), it can be made arbitrarily small by choosing suitably large integers $N, N_\pm$. In both methods we obtain, as long as $\Delta < 0.1$, fairly stable and consistent results, which converge to the same limit for large $N, N_\pm$, where Δ vanishes and full incommensurability is restored. In a $(r_+, r_- = r_+^2)$ scheme, the speed of convergence depends crucially on the nature of the incommensurability of r_+. Quadratic irrational values of r_+ are, thanks to their *periodic* continued-fraction representation [7], especially advantageous and yield a rapidly vanishing phase error $\Delta \propto N^{-1}$ (the example quadratic irrationals of figure 1(b) include the golden mean $\phi = (1+\sqrt{5})/2 \simeq 1.618$, with continued-fraction coefficients $(1, 1, 1, \ldots)$, and $(2+\sqrt{2})/3 \simeq 1.138$, with continued-fraction coefficients $(1, 7, 4, 8, 4, 8, 4, 8, \ldots)$). By contrast, for non-quadratic irrationals, and/or for general $r_- \neq r_+^2$, the phase error vanishes much more slowly, $\Delta \propto N^{-1/2}$ (the examples of figure 1(b) include the spiral mean $\sigma \sim (1, 3, 12, 1, 1, 3, 2, 3, 2, 4, \ldots) \simeq 1.325$ solution of $\sigma^3 = \sigma + 1$, and $\pi/2 \sim (1, 1, 1, 3, 31, 1, 145, 1, 4, 2, \ldots) \simeq 1.571$). Finally, for the class $(r_+,\ r_- = \theta r_+/[r_+ - 1])$, with rational θ, the error decays rapidly $\Delta \propto N^{-1}$, regardless of the irrational nature of r_+.

Finite chains with open boundary conditions (OBC) were also considered, with similar results briefly discussed below, and dealt with in greater detail in [8]. Similar models were considered in the past [9–11], missing however the ingredient of incommensurability, which is important for the novel features shown here. A previous study of the present model [12] achieved the sliding through application of driving to one of the two substrates, via an *additional spring*. That procedure obscures the quantization phenomena, which are instead uncovered when sliding occurs with a constant *velocity* $v_{\rm ext}$.

Upon sliding the substrates, $v_{\rm ext} \neq 0$, the lubricant chain slides too. However, it generally does so in a nontrivial manner: the time-averaged relative chain velocity, $w = v_{\rm cm}/v_{\rm ext}$, is generally *asymmetric*, namely different from $1/2$. Even more surprisingly, w is exactly *quantized*, for large parameter intervals, to plateau values that depend solely on the chosen commensurability ratios. The asymmetrical w-plateaus are generally very stable, and insensitive to many details of the model, indicating an intrinsically topological nature. We show that they are the manifestation of a certain density of topological solitons (*kinks*) in the lubricant versus the 'denser' substrate potential with periodicity a_+. These solitons are set into motion with the external driving velocity $v_{\rm ext}$ by the sliding 'sparser' substrate with periodicity a_-.

2. The plateau dynamics

We now turn to illustrating the results. We integrate the equations of motion (1), starting from fully relaxed springs ($x_i = \mathrm{i}a_0$, $\dot{x}_i = v_{\rm ext}/2$), by a standard fourth-order Runge–Kutta method. After an initial transient, the system reaches its dynamical stationary state, at least so long as γ is not exactly zero. Figure 2(a) shows the resulting time-averaged centre-of-mass (CM)

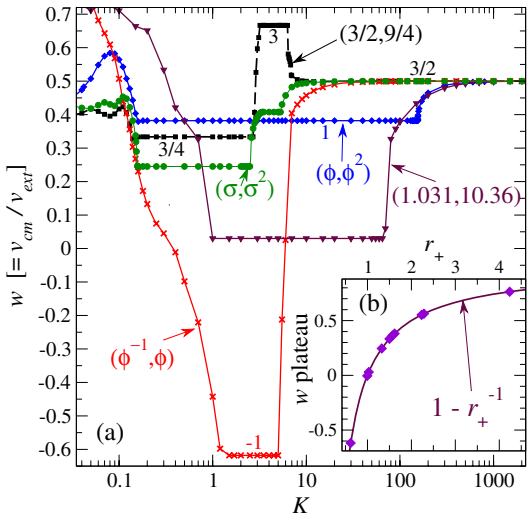

Figure 2. (a) Average drift velocity ratio $w = v_{\rm cm}/v_{\rm ext}$ of the chain as a function of its spring stiffness K for different length ratios (r_+, r_-): commensurate $(3/2, 9/4)$, golden mean (GM) (ϕ, ϕ^2), spiral mean (σ, σ^2), r_+ close to unity $(\frac{1031}{1000}, \frac{1031}{1000}\sqrt{101}) \simeq (1.031, 10.36)$—dilute kinks, and r_+ smaller than unity (ϕ^{-1}, ϕ)—antikinks. When relevant, plateaus are labelled by the rational θ of equation (6). All simulations are carried out in PBC with $\gamma = 0.1$, $v_{\rm ext} = 0.1$. The (ϕ, ϕ^2) plateau value is $w = 0.381\,966\ldots$, identical to $1 - \phi^{-1}$ to eight decimal places. (b) The main plateau speed w as a function of r_+.

velocity $v_{\rm cm}$ as a function of the chain stiffness K for five representative (r_+, r_-) values: three with $r_+ > 1$ and $r_- = r_+^2$, one with unrelated r_+, r_- and one with $r_+ < 1$. We find that $w = v_{\rm cm}/v_{\rm ext}$ is generally a complicated function of K, with flat plateaus and regimes of continuous evolution, in a way which is qualitatively similar for different cases. The main surprise is that all plateaus show perfectly flat w values that are exactly constant (quantized) to all figures of numerical accuracy, the precise value strikingly independent of K, of γ, of $v_{\rm ext}$, and even of F_-/F_+.

To explore the origin of the w plateaus, we analyse the dynamics for a large number of values of (r_+, r_-), and observe that: (i) at least one velocity plateau as a function of K occurs for a wide range of (r_+, r_-); (ii) additional narrower secondary plateaus often arise for a stiffer chain (larger K, see figure 2(a)); (iii) the velocity ratio w of the main plateau—the first plateau found for increasing K—satisfies

$$w = 1 - r_+^{-1}, \tag{3}$$

for a large range of (r_+, r_-); see figure 2(b).

As sketched in our recent note [3], we can understand these results as follows. Consider for illustration a situation of quasi-commensuration of the chain to the a_+ substrate: $r_+ = 1 + \delta$, with $\delta \ll 1$. The slight commensurability mismatch induces a density

$$\rho_{\rm sol} = \frac{\delta}{a_+} = \frac{r_+ - 1}{a_+} \tag{4}$$

of solitons (or kinks), essentially substrate minima holding two particles, rather than one [1]. Assume that the second, less oscillating a_- slider, which moves at velocity $v_{\rm ext}$, will *drag* the kinks along: $v_{\rm sol} = v_{\rm ext}$. If $\rho_0 = 1/a_0 = r_+/a_+$ is the linear density of lubricant particles, mass

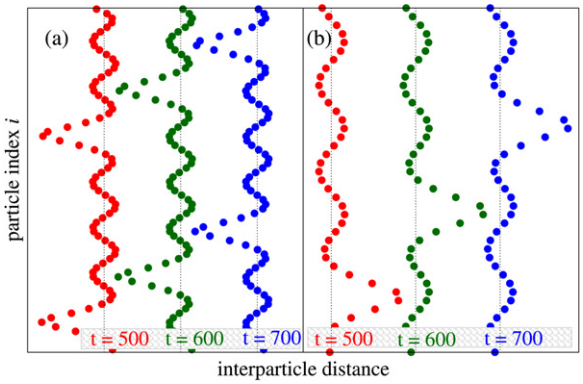

Figure 3. Snapshots of the distance between neighbouring lubricant particles in the chain $x_i - x_{i-1}$ at three successive time frames. All simulations are carried out with $\gamma = 0.1$, $v_{\rm ext} = 0.1$, $r_- \simeq 10.36$, and $K = 10$ (inside the main plateau): (a) $r_+ = 1.031$ (kink density $\delta/a_+ = 0.031/a_+$); (b) $r_+ = 0.995$ (anti-kink density $|\delta|/a_+ = 0.005/a_+$).

transport will obey $v_{\rm cm}\rho_0 = v_{\rm sol}\rho_{\rm sol}$. This yields precisely

$$w = \frac{v_{\rm cm}}{v_{\rm ext}} = \frac{\rho_{\rm sol}}{\rho_0} = \frac{\delta}{r_+} = 1 - \frac{1}{r_+}. \tag{5}$$

Thus the quantized velocity plateaus appear to arise because the smoother slider (whose exact period a_- is irrelevant, but is the one further away from the chain's periodicity, $r_- > r_+$) drags the lattice of kinks, of fixed and given density, at its own full external speed $v_{\rm ext}$, as illustrated in figure 3(a). As shown in figure 2(b), the physics of kink dragging is not limited to the quasi-commensurate case $\delta \ll 1$, but extends to all values of $|\delta| \sim 1$, where individual kinks can hardly be singled out. Amusingly, this mechanism also works for $\delta < 0$, i.e. $r_+ < 1$. Here kinks are replaced by anti-kinks, and we find that the chain moves in the *opposite* direction to the external driving $v_{\rm ext}$ ($w < 0$; see figure 2(a) for $r_+ = \phi^{-1}$). Exactly as holes in a semiconductor, anti-kinks (carrying a negative 'charge') dragged at velocity $+v_{\rm ext}$ effectively produce a *backward* net motion of the lubricant layer. This 'upstream' motion of the anti-kinks (regions of increased inter-particle separation, and of decreased local particle density) is illustrated in figure 3(b).

Before moving on, we must explain what makes the chain select the substrate with which kinks are formed, as opposed to the other substrate merely acting as a moving brush dragging the kinks along. As it turns out, kinks are formed relative to the nearer-in-register substrate, which, by construction, here has the period a_+. The density (4) of kinks is such that they can be either commensurate or incommensurate relative to the periodicity a_- of the second substrate. The soliton lattice is commensurate to the a_- substrate whenever the ratio of a_- to the average inter-kink distance $\rho_{\rm sol}^{-1}$ is a rational number θ, i.e. when

$$r_- = \frac{r_+}{r_+ - 1}\theta. \tag{6}$$

We find that this condition, for $\theta = 1$, is particularly beneficial to the formation of a large and stable main plateau. Indeed, $(r_+, r_-) = (\phi, \frac{\phi}{\phi-1}) = (\phi, \phi^2)$ does satisfy equation (6) for $\theta = 1$, and its K-plateau covers almost three decades, as shown in figure 2(a). We find similarly wide plateaus for $(r_+, \frac{r_+}{r_+-1})$, with $r_+ = \sigma$, $r_+ = \pi/2$ and $r_+ = \pi^{1/2}$.

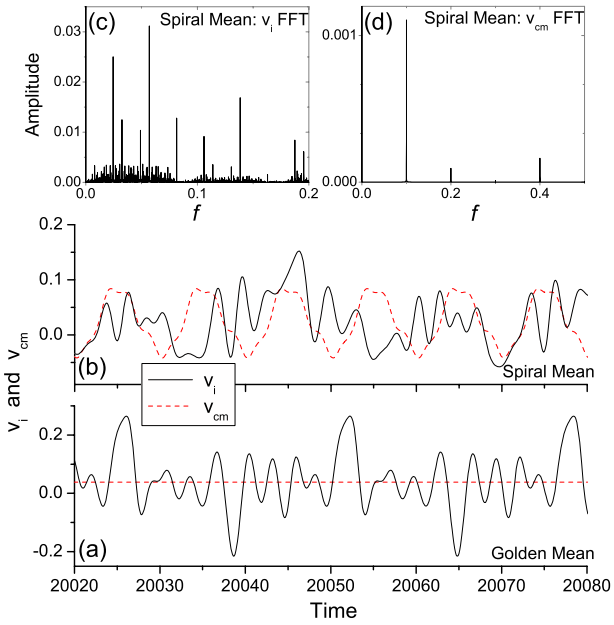

Figure 4. Time evolution of a particle velocity $\dot{x}_i$, and of the chain CM velocity $v_{\rm cm}$ (fluctuations rescaled by a factor 50), for the GM (a) and SM (b) cases of figure 2. Amplitudes of the Fourier spectrum of $\dot{x}_i(t)$ (c) and of $v_{\rm cm}(t)$ (d) for $r_+ = \sigma$. Individual particle spectra have identical amplitudes, and differ only in the phases, which leads to a remarkable cancellation in the $v_{\rm cm}$ power spectrum. Here $K = 1$, $\gamma = 0.1$, and $v_{\rm ext} = 0.1$.

2.1. Individual particle motion and CM periodic dynamics

The motion of the individual particles is also very instructive. Figure 4 shows the time evolution of the velocity of a single chain particle $\dot{x}_i$, and of $v_{\rm cm}$, for a value of K inside a plateau, $K = 1$, for $r_+ = \phi$ and $r_+ = \sigma$ of figure 2. Here two clear kinds of behaviour emerge. The single-particle motion of each particle in the chain is, during motion in the GM plateau, perfectly time-periodic. A similar periodic dynamics is found, in appropriate regimes, for all rational and *quadratic* irrational ($r_+, r_- = r_+^2$) values that we tested. Similarly, periodic motion emerges on the plateaus of (r_+, r_-) satisfying equation (6), for arbitrary r_+. In contrast, single-particle motion in the (σ, σ^2) spiral mean (SM) case is definitely not periodic. The Fourier spectrum of the particle motion, shown in figure 4(c), confirms that SM sliding yields only quasi-periodic orbits with two prominent incommensurate frequencies f_+ and f_-, which can be interpreted as the average frequency of encounter of a generic particle with the two substrate periodic corrugations, $f_+ = v_{\rm cm}/a_+$ and $f_- = (v_{\rm ext} - v_{\rm cm})/a_-$, respectively. There is, however, a complete and exact phase cancellation between the Fourier spectra of different chain particles (all having the same amplitude spectrum, with different phases), giving rise to a strictly periodic motion of the chain CM even in the SM case. Periodic CM velocity oscillations around an exactly quantized drift velocity is a common and generic feature of all plateaus in the chain dynamics. These periodic oscillations can be understood as the solitons moving at velocity $v_{\rm ext}$ encountering the periodic Peierls–Nabarro potential [1] of period a_+. The corresponding frequency of encounter $v_{\rm ext}/a_+$ is clearly visible in figure 4(d). We observe that the Peierls–Nabarro barrier vanishes (yielding a strictly constant $v_{\rm cm}$) for all cases where the particle motion is periodic, particularly all (r_+, r_-) satisfying equation (6). When such a

periodic single-particle motion occurs for a a_--commensurate soliton lattice, equation (6), the frequency ratio

$$\frac{f_+}{f_-} = r_- \frac{(r_+ - 1)}{r_+} = \theta. \tag{7}$$

As this condition is equivalent to equation (6), this analysis attributes to the rational θ the double significance of (i) the coverage fraction of solitons on the substrate of periodicity a_-, and (ii) the ratio between the average frequencies f_+ and f_- of encounter of the features of the two substrates.

Low driving velocities $v_{\rm ext}$ are beneficial to the appearance and to the width of velocity plateaus. For increasing $v_{\rm ext}$, the plateaus shrink and eventually disappear, still remaining exact while they do so. The critical $v_{\rm ext}$ where the plateaus eventually disappear depends on K, but is usually smaller than unity, for the parameters of figure 2. Fully commensurate $\theta = 1$ plateaus such as that of the (ϕ, ϕ^2) case are especially wide and robust against an increase in $v_{\rm ext}$ (for the parameters of figure 2 and $K = 4$, up to $v_{\rm ext} \simeq 1.5$) and other perturbations. Within the class of (r_+, r_+^2) length ratios, $r_+ = \phi$ appears therefore, in the present dynamical context, as the 'most *commensurate*' irrational, which is at variance with static pinning in the standard FK model, where the opposite occurs [1, 13].

All the above is for PBC. As anticipated, OBC simulations [8] show, however, that the PBC that are used are not crucial to the plateau quantization, which occurs even for a lubricant 'patch' of finite and not particularly large size N, perhaps such as a hydrocarbon chain molecule in one dimension (1D) or an interposed graphite flake in two dimensions (2D). The finite lubricant size does not remove the plateaus. On the contrary, it permits and favours the development of robust velocity plateaus as a function of stiffness. The plateau values are not identical to those of the infinite chain with PBCs. The reason for that is that finite size allows for an overall chain-length re-adjustment which spontaneously promotes single-particle *periodic* oscillations, effectively satisfying equation (6).

2.2. Dynamical incompressibility and tribological dissipation

Returning to the general infinite chain case, the finding of exact plateaus implies a kind of 'dynamical incompressibility', namely identically null response to perturbations or fluctuations trying to deflect the CM velocity away from its quantized value. In order to probe the robustness of the plateau attractors, we can introduce an additional constant force F acting on all particles in the chain, whose action is to try to alter the force-free sliding velocity away from its plateau value. As expected, as long as F remains sufficiently small, it does perturb the single-particle motions but has no effect whatsoever on w, which remains exactly pinned to the attractor ($v_{\rm cm} \equiv v_{\rm plateau}$). The plateau dynamics is only abandoned above a critical force $F_{\rm c}$. This dynamical depinning takes place through a series of type-I intermittencies [14], as shown in figure 5(b) where $v_{\rm cm}(t)$ is plotted against a slow adiabatic ramping of F.

A precise value of $F_{\rm c}$ can be obtained by ramping F with time with a gentle enough rate of increase or, alternatively, by a Floquet–Lyapunov linear stability analysis. This procedure is standard [15] and amounts to studying the eigenvalues of a $2N \times 2N$ matrix $\mathbf{R}$ whose columns are the linearized time evolutions, over one period T, of the standard basis vectors $\mathbf{e}_i = \delta_{i,j}$ in phase space. The motion is stable if the (complex) eigenvalues ν_i of $\mathbf{R}$ are smaller than unity, $|\nu_i| < 1$; intermittencies of type I arise when the largest (in modulus) eigenvalue of $\mathbf{R}$, $\nu_{\rm max}$, reaches the point 1 in the complex plane, $\nu_{\rm max} \to 1$, which is indeed what we find at the edge of the GM plateau. The value of $F_{\rm c}$ is a function of the parameters, and $F_{\rm c}$ vanishes linearly when K approaches the border $K_{\rm c}$ of the plateau, as in figure 5(a). The depinning transition line $F_{\rm c}$ shows a jump Δv in the average $v_{\rm cm}$ and a clear hysteretic behaviour [16] as F crosses

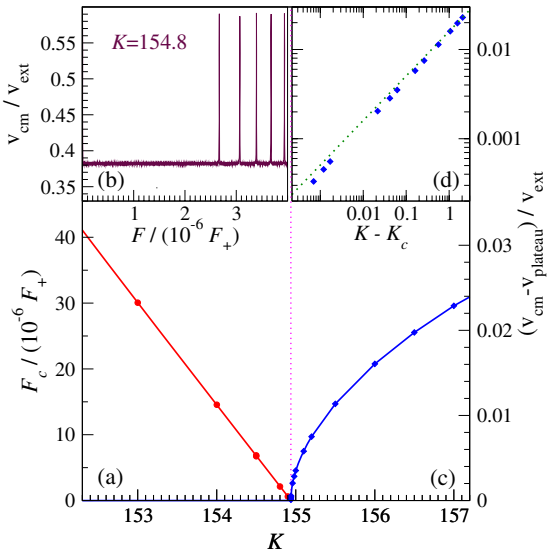

Figure 5. Dynamical depinning force F_c for the GM plateau (a), extracted by a slow adiabatic increase of the force F applied to all particles, until intermittencies appear, signalling collective slips (b). The critical behaviour of the average velocity for $K \to K_c$ ((c), (d)), showing the typical square-root singularity (dotted line) associated with type-I intermittencies. Here $\gamma = 0.1$ and $v_{ext} = 0.1$ were used.

F_c, for not too large values of $K < K_c$. As can be expected, Δv decreases to 0 as K increases. Around $K = K_c$ the depinning transition is continuous. The specific point $K = K_c$ represents the zero-F crossing of the depinning line, which extends to negative F above K_c. The precise value of K_c depends on parameters such as v_{ext} and γ. As K approaches K_c from above (no external force), v_{cm} approaches $v_{plateau}$ in a critical manner, as suggested in figure 2(a). This is detailed in figures 5(c) and (d), where the critical behaviour is shown to be $\Delta v \propto (K - K_c)^{1/2}$, the value typical of intermittencies of type I [14]. For $K > K_c$, in fact the chain spends most of its time moving at $v_{cm}(t) \simeq v_{plateau}$, except for short bursts at regular time intervals τ, where the system as a whole jumps ahead by a_0, i.e. an extra chain lattice spacing (collective slip). The characteristic time τ between successive collective slips diverges as $\tau \propto (K - K_c)^{-1/2}$ for $K \to K_c$, consistent with the critical behaviour of w. We verified that the w-plateaus for more general values of r_+ and of r_- show the same kind of infinite stiffness, and a critical decrease of F_c near the plateau edge, similar to that of figure 5(a) for the GM.

We have investigated the *tribological* properties of the model in the plateau regime. As the dissipative term makes no work on particles that move at velocity $\dot{x}_i = v_{ext}/2$, it is particularly convenient to evaluate the dissipated power in the 'symmetric' frame of reference where the upper chain moves at velocity $\frac{v_{ext}}{2}$ and the lower chain moves at velocity $-\frac{v_{ext}}{2}$. In this frame of reference, the instantaneous total power dissipated by the γ term amounts to

$$P = \sum_i \dot{x}_i \cdot (2\gamma \dot{x}_i) = 2\gamma \sum_i \dot{x}_i^2 = \frac{4\gamma}{m} E_{kin}, \tag{8}$$

where E_{kin} is the total kinetic energy of the particles in the symmetric frame of reference. This power fluctuates, but eventually, in the dynamical stationary state, its average value $\langle P \rangle$ equals on average the mean power necessary to maintain the motion of the sliders [12]. Figure 6 shows the dissipated power per particle in a wide range of K values for the (ϕ, ϕ^2) model. It is

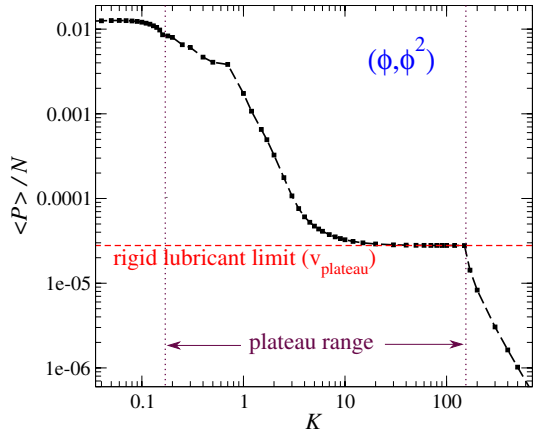

Figure 6. The average dissipated power per particle for the GM $(r_+, r_-) = (\phi, \phi^2)$ model as a function of the spring stiffness K. All dynamical parameters are as in figure 2. Two dotted lines indicate the plateau range. A dashed horizontal line marks the theoretical lowest dissipation limit of a rigid lubricant in a purely translational motion at speed $v_{\rm plateau} = (1 - \phi^{-1})\, v_{\rm ext}$.

apparent that the friction decreases as the springs become stiffer and stiffer, where fluctuations are of decreasing amplitude. The plateau region does not appear to be especially conspicuous in this frictional decrease, except for a net drop at the end of the plateau, due to the lubricant moving closer and closer to the symmetric velocity $v_{\rm ext}/2$.

3. Conclusions

The phenomena just described for a model 1D system might have 2D counterparts, potentially observable in real systems. Nested carbon nanotubes [17], or confined one-dimensional nanomechanical systems [18], are one of several possible arenas for the phenomena described in this paper. Though speculative at this stage, an obvious question is what aspects of the phenomenology just described might survive in 2D, where tribological realizations, such as the sliding of two hard crystalline faces with, for example, an interposed graphite flake, are conceivable. Our results suggests that the lattice of discommensurations—a Moiré pattern—formed by the flake on a substrate could be dragged by the other sliding crystal face, in such a manner that the speed of the flake as a whole would be smaller, and quantized. This would amount to the slider 'ironing' the solitons onward. Dienwiebel *et al* [19] demonstrated how incommensurability may lead to virtually friction-free sliding in such a case, but no measure was obtained for the flake's relative sliding velocity. Unlike our model, real substrates are neither rigid nor ideal, but subject to thermal expansion and characterized by defects. Nevertheless, the ubiquity of plateaus shown in figure 2, and their topological origin, suggest that these effects would not remove the phenomenon. A real-life situation with a distribution of differently oriented crystalline micro-grains, each possessing a different incommensurability, is also potentially interesting; each grain, we expect, will tend to stabilize a certain average CM velocity, depending on its incommensurability. Other realizations or applications inspired by the physics described by our model might be accessible, notably in grain-boundary motion, in the sliding of optical lattices [20] or of charge-density-wave systems [21].

Acknowledgments

We are grateful to O M Braun for invaluable discussions. This research was partially supported by PRRIITT (Regione Emilia Romagna), Net-Lab 'Surfaces & Coatings for Advanced

Mechanics and Nanomechanics' (SUP&RMAN) and by Ministero Italiano dell'Università e della Ricerca (MIUR) Cofin 2004023199, Fondo per gli Investimenti della Ricerca di Base (FIRB) RBAU017S8R, and RBAU01LX5H.

References

[1] Braun O M and Kivshar Yu S 2004 *The Frenkel–Kontorova Model: Concepts, Methods, and Applications* (Berlin: Springer)
[2] Kapitaniak T and Wojewoda J 1993 *Attractors of Quasiperiodically Forced Systems* (Singapore: World Scientific)
[3] Vanossi A, Manini N, Divitini G, Santoro G E and Tosatti E 2006 *Phys. Rev. Lett.* **97** 056101
[4] Santoro G E, Vanossi A, Manini N, Divitini G and Tosatti E 2006 *Surf. Sci.* **600** 2726
[5] van Erp T S, Fasolino A, Radulescu O and Janssen T 1999 *Phys. Rev.* B **60** 6522
[6] Vanossi A, Röder J, Bishop A R and Bortolani V 2000 *Phys. Rev.* E **63** 017203
[7] Khinchin A Ya 1997 *Continued Fractions* (New York: Dover)
[8] Cesaratto M, Manini N, Vanossi A, Tosatti E and Santoro G E 2007 *Surf. Sci.* submitted
(Cesaratto M, Manini N, Vanossi A, Tosatti E and Santoro G E 2006 *Preprint* cond-mat/0609116)
[9] Filippov A E, Klafter J and Urbakh M 2001 *Phys. Rev. Lett.* **87** 275506
[10] Rozman M G, Urbakh M and Klafter J 1996 *Phys. Rev. Lett.* **77** 683
Rozman M G, Urbakh M and Klafter J 1997 *Europhys. Lett.* **39** 183
[11] Zaloj V, Urbakh M and Klafter J 1998 *Phys. Rev. Lett.* **81** 1227
[12] Braun O M, Vanossi A and Tosatti E 2005 *Phys. Rev. Lett.* **95** 026102
[13] Peyrard M and Aubry S 1983 *J. Phys. C: Solid State Phys.* **16** 1593
[14] Bergé P, Pomeau Y and Vidal C 1984 *Order Within Chaos* (Paris: Hermann and Wiley)
[15] José J V and Saletan E J 1998 *Classical Dynamics: A Contemporary Approach* (Cambridge: Cambridge University Press)
[16] Vanossi A, Santoro G E, Manini N, Cesaratto M and Tosatti E 2007 *Surf. Sci* submitted
(Vanossi A, Santoro G E, Manini N, Cesaratto M and Tosatti E 2006 *Preprint* cond-mat/0609117)
[17] Zhang X H, Tartaglino U, Santoro G E and Tosatti E 2007 *Surf. Sci.* at press
[18] Toudic B, Aubert F, Ecolivet C, Bourges P and Breczewski T 2006 *Phys. Rev. Lett.* **96** 145503
[19] Dienwiebel M, Verhoeven G S, Pradeep N, Frenken J W M, Heimberg J A and Zandbergen H W 2004 *Phys. Rev. Lett.* **92** 126101
[20] Bloch I 2005 *Nat. Phys.* **1** 23
[21] Grüner G 1988 *Rev. Mod. Phys.* **60** 1129